RSC Advances

PAPER

View Article Online
View Journal | View Issue

Cite this: *RSC Adv.*, 2021, **11**, 12703

Effect of relative percentage of acid and base sites on the side-chain alkylation of toluene with methanol

Huijun Li,†[a] Bin Wang,†[a] Yueli Wen,*[b] Chunyao Hao,[a] Yuhua Liu[a] and Wei Huang*[ac]

Received 12th January 2021
Accepted 19th March 2021

DOI: 10.1039/d1ra00263e

rsc.li/rsc-advances

K_3PO_4/NaX catalysts were prepared by loading potassium phosphate on NaX zeolite, and the catalytic performance was studied for the side-chain alkylation of toluene with methanol to styrene and ethylbenzene. Combined with the characterization of XRD, TPD-NH_3, TPD-CO_2, and FTIR and the determination of phosphorus content, it is revealed that firstly, the P element loaded on the catalyst surface can prominently promote the percentage of middle base sites, which will accordingly enhance the selectivity of the products (styrene and ethylbenzene) of side-chain alkylation of toluene; secondly, if there are enough middle base sites distributed on the catalysts, the higher percentage of strong base sites benefit the selectivity of styrene, which is confirmed by the performance of the two-stage catalysts.

1 Introduction

In 1967, Sidorenko *et al.* first reported that side-chain alkylation of toluene with methanol could form styrene and ethylbenzene on an alkali-metal modified X-zeolite catalyst,[1] and thereafter researchers around the world followed this discovery. Recently, extensive efforts have been made on studying the reaction mechanism of the side-chain alkylation of toluene. It is well known that side-chain alkylation of toluene with methanol (SCAT) is an acid–base synergistic catalysis process.[2–4] During the toluene side-chain alkylation process, the main reaction networks occur as follows:

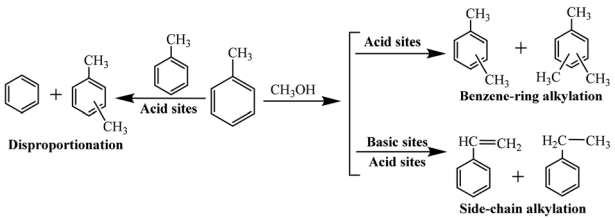

For the SCAT reaction, it is worth noting that both the base and acid sites are necessary. The base sites are in charge of absorbing and stabilizing toluene, while the acid sites are responsible for activating the C–H bonds on the side chain of toluene and dehydrogenation of methanol to formaldehyde.[5,6] Otherwise, in this process, the formation of xylene by disproportionation of toluene and the benzene-ring alkylation of toluene will occur on acid sites.[7] In addition, strong basic sites are required for the abstraction of H^+ from toluene. However, very strong basic sites would promote the formation of formaldehyde from methanol, and formaldehyde would further decompose into carbon monoxide and hydrogen.[8] Furthermore weak basic sites could only promote the dehydrogenation of methanol to formaldehyde without abstracting H^+ from toluene. So it is very meaningful to discover the optimal acid–base property and amount of acid and base sites for side-chain alkylation of toluene with methanol.

In the study of catalysts for this reaction, most of the research has concentrated on the modification of various zeolites with alkali metals, alkaline earth metals and other promoters to adjust the acidity and alkalinity of the catalysts. Quite a lot of types of catalysts have been investigated for SCAT so far, like X zeolite catalysts modified with different composites (such as alkali earth metal,[9,10] rare earth metal,[11] transition metal,[12–15] boron[16,17] and phosphorus[18–20]), metal oxide catalysts,[21,22] layered double hydroxides (LDHs),[23,24] N-doped catalysts[25,26] and other alkaline catalysts, in which X zeolite[27–29] modified with alkaline metal showed the superior catalytic performance. Our group has prepared K_3PO_4/CsX catalysts and used for SCAT, and it was found that the moderate addition of K_3PO_4 could decrease the amount of weak acid sites and increase the amount of middle base sites. Herein, in order to discover how the acid/base sites affect the catalytic performance

[a]*Key Laboratory of Coal Science and Technology of Ministry of Education and Shanxi Province, Taiyuan University of Technology, Taiyuan 030024, Shanxi, China. E-mail: huangwei@tyut.edu.cn*

[b]*College of Environmental Science and Engineering, Taiyuan University of Technology, Taiyuan, Shanxi 030024, China. E-mail: wenyueli@tyut.edu.cn*

[c]*Coal Conversion Technology & Engineering Co., Ltd., Taiyuan University of Technology, Taiyuan, 030024, Shanxi, China*

† Huijun Li and Bin Wang are co-first authors who have equally contributed to this work.

for SCAT, a series of K_3PO_4/NaX catalysts were prepared and the effect of the relative percentage of acid/base sites on this catalytic reaction were investigated in this work.

2 Experimental

2.1 Materials

All reagents including methanol, methylbenzene, potassium hydroxide, potassium phosphate, anhydrous ethanol were all of analytical grade (purchased from Tianjin Kemiou Chemical Reagent Co. Ltd of China) and were used without further purification. NaX zeolite (Si/Al = 1.25) were purchased from Tianjin Nankai University. Distilled water was used in all experiments without further treatment.

2.2 Catalyst preparation

2.2.1 Preparation of pro-catalyst. A series of catalysts were prepared by a repeated impregnation–washing method. The specific process was described as follows: 10 g NaX zeolite was ion-exchanged in different concentrations of K_3PO_4 solution (solid/liquid ratio, 10 g/100 mL) three times at 80 °C for 2 h. After separated from the slurry by using Buchner funnel and washed twice with a 0.01 mol L^{-1} solution of K_3PO_4, the obtained solid was dried at 80 °C overnight, and then calcined at 500 °C for 3 h. Finally, the collected white powder, as the pro-catalyst, was named as Cat-*n*, *n* is the concentration of K_3PO_4 solution.

2.2.2 Preparation of co-catalyst. 10 g NaX zeolite was modified with KOH solutions of different concentrations by incipient wetness impregnation. The loading amount of potassium hydroxide was controlled by the concentration of potassium hydroxide aqueous solution. The obtained solid were dried at 80 °C overnight, and then calcined at 500 °C for 3 h. The co-catalysts were named as *m*%KOH/NaX, *m* represented the weight percentage of KOH.

In order to discover how the strong base sites affect the side-chain alkylation of toluene with methanol to styrene, the co-catalyst was placed in front of pro-catalyst, separated by quartz wool.

2.3 Catalyst characterization

The powder X-ray diffraction (XRD) patterns were collected on a Rigaku D/Max-2500 ($\lambda = 0.1542$ nm) diffractometer with a Ni-filtered Cu Kα radiation source operating at 40 kV and 100 mA. The angle 2θ were recorded from 5° to 85° with a scanning rate of 8 min^{-1}. Temperature-programmed desorption (TPD) was carried out using CO_2 or NH_3 as probe molecules. The procedures were as follows: 100 mg of fresh catalyst was preprocessed at 450 °C under He stream for 30 min and then cooled down to 50 °C. CO_2 or NH_3 was infused into the stream at 50 °C for 30 min. The physically adsorbed CO_2 or NH_3 was removed by He stream at 50 °C for 1 h. Then the catalyst was heated from 50 °C to 850 °C in He stream at a heating rate of 10 °C min^{-1}, and the desorbed gas was detected by a thermal conductivity detector at the same time. Determination of P elements content in the catalysts was based on Chinese Standard GB175-1999 by using ultraviolet-visible (UV-vis) spectrophotometer. Fourier transform infrared spectroscopy (FTIR) were recorded on a Bio-Rad FTS-60A spectrometer with the KBr wafer technique.

2.4 Catalysis reaction and products analysis

The evaluation of catalysis activity for side-chain alkylation of toluene with methanol was carried out at atmospheric pressure in a stainless steel fixed-bed reactor. In order to prevent blockage happening in the reactor, the catalysts were granulated to 40–60 mesh. The catalyst sample (0.9 g) was firstly activated at 450 °C for 2 h under a flow of N_2 and then cooled down to 425 °C, the desired reaction temperature. The liquid mixture of toluene and methanol with a molar ratio of 5 : 1 was pumped into the reactor using a peristaltic pump at a rate of 0.6 mL h^{-1}, the vaporized reactants were diluted by flowing nitrogen stream (3 mL min^{-1}). After the catalysts reached steady state, the reaction products were analyzed by an on-line gas chromatograph (GC950, China Shanghai HaiXin Chromatographic Instruments Co. Ltd) with a flame ionization detector (FID) using an FFAP capillary column (0.53 mm × 50 m).

The conversion of methanol, selectivity and yield of the products (S_X and Y_X) were defined in the following equations:

$$C_{Meth} = \left(1 - \frac{\text{methanol outlet}}{\text{methanol inlet}}\right) \times 100\%$$

$$S_X = \left(\frac{X}{\text{methanol inlet} - \text{methanol outlet}}\right) \times 100\%$$

$$Y_X = S_X \times C_{Meth}$$

3 Results and discussion

3.1 Catalyst characterization

3.1.1 XRD analysis. The XRD patterns of different catalysts are exhibited in Fig. 1. All the samples showed sharp XRD peaks at 6.2°, 23.4°, 26.7° and 31.0°, which has almost the same diffraction pattern with NaX without ion-exchange (Cat-0) and can be attributed to the characteristic peaks of faujasite zeolite structure. In addition, the characteristic diffraction peaks of the zeolite after ion-exchange are weak overall as compared to the NaX (Cat-0). A possible reason is that part of the zeolite structure was slightly damaged during the ion-exchange process, which has been discovered by many researchers. It is worth mentioning that the diffraction peak intensity at 31.8°, which can be assigned to K_3PO_4 phase (PDF no. 20-0921), increases when the concentration of K_3PO_4 aqueous solution is more than 0.25 mol L^{-1}. This phenomenon may be due to the surface deposition of K_3PO_4 with well-structured crystal on the NaX zeolite when aqueous solution concentration is relatively large. When the concentration of K_3PO_4 solution is less than 0.25 mol L^{-1}, the K_3PO_4 species can be highly dispersed and

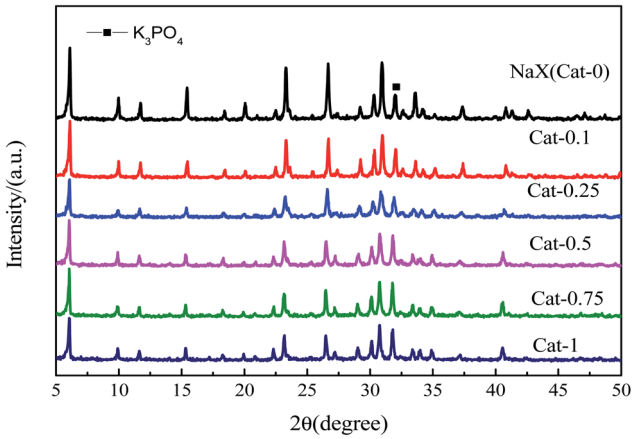

Fig. 1 XRD patterns of the catalysts NaX (Cat-0), Cat-0.1, Cat-0.25, Cat-0.5, Cat-0.75 and Cat-1.

interact well with NaX zeolite, in which K_3PO_4 doesn't exhibit good crystal structure.

3.1.2 FTIR analysis. In order to discover the functional group and the compositions that presence in Cat-*n* catalysts, the Fourier transform infrared spectroscopy (FTIR) was used. As shown in Fig. 2, the strong absorption peaks at 3468 cm^{-1} and 1645 cm^{-1} can be observed, which are attributed to the O–H bending vibrations of absorbed water. The absorption peaks at 968 cm^{-1}, 741 cm^{-1} and 670 cm^{-1} are assigned to the asymmetric and symmetric stretching vibrations of tetrahedrons in NaX zeolite structure. Among them, the main peak appearing at 968 cm^{-1} belongs to the asymmetric telescopic vibration peak, and the other two absorption peaks at 741 cm^{-1} and 670 cm^{-1} are weaker, which correspond to the symmetrical telescopic vibration peak. The spectra of the catalysts are almost the same as the characteristic absorption spectra of NaX zeolite.[30] The stretching vibration peak of P=O was found at 1371 cm^{-1} in the catalyst obtained by ion exchange with the K_3PO_4 solution compared to NaX. When the concentration of K_3PO_4 solution is larger than 0.1 mol L^{-1}, a weak absorption peak appears at

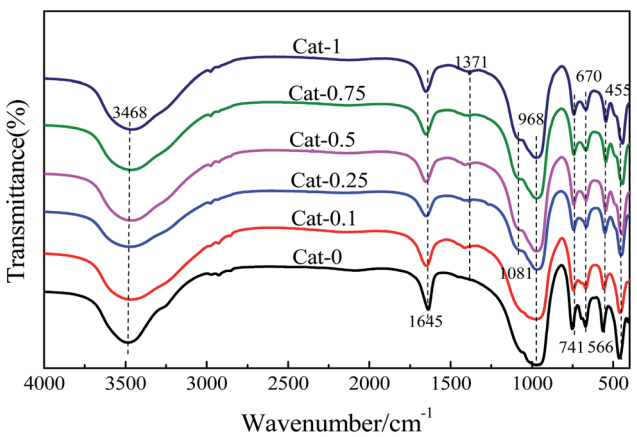

Fig. 2 FTIR spectra of the catalysts NaX (Cat-0), Cat-0.1, Cat-0.25, Cat-0.5, Cat-0.75 and Cat-1.

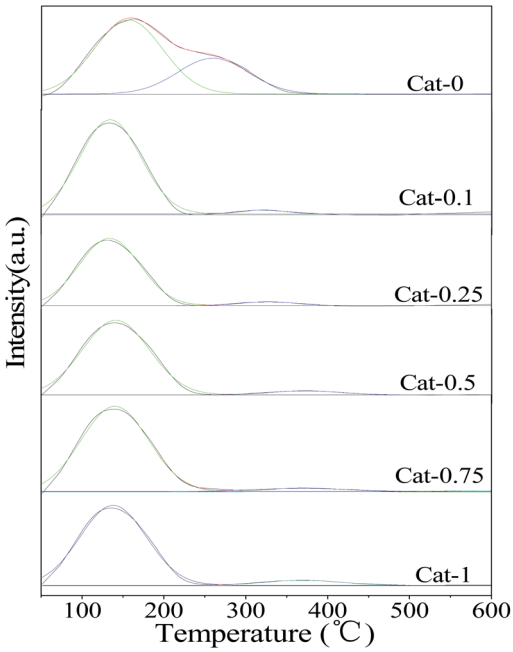

Fig. 3 Profiles of NH_3-TPD for the catalysts Cat-0, Cat-0.1, Cat-0.25, Cat-0.5, Cat-0.75 and Cat-1.

1081 cm^{-1}, which belongs to the P–O vibration of K_3PO_4. This indicated that when K_3PO_4 with higher concentrations were used as an exchange solution, some of the PO_4^{3-} ions could be loaded on the catalyst.

3.1.3 TPD analysis. The NH_3-TPD curves of the catalysts are showed in Fig. 3. All the samples have two desorption peaks at the range of 50–200 °C and 200–500 °C, which correspond to the weak and middle acid sites respectively. Furthermore, the areas of desorption peaks were integrated, the relative percentage of the weak and middle acid sites were calculated by the integral areas shown in Table 1. It is found that the presence of K_3PO_4 makes the percentage of middle acid sites decreased obviously on the catalysts, but the concentration of K_3PO_4 solution has less effect on the distribution of different types of acid sites on the catalyst.

The CO_2-TPD curves of Cat-*n* catalysts after the ion-exchanged are shown in Fig. 4. It can be seen that all the samples have three isolated desorption peaks zones: the first one in the range of 50–250 °C belongs to weak base sites, the second one in 250–500 °C can be attributed to middle base sites,

Table 1 Distribution of different types of acid sites on the catalyst

Catalyst	Weak/all (%)	Middle/all (%)
Cat-0	67	33
Cat-0.1	97	3
Cat-0.25	95	5
Cat-0.5	95	5
Cat-0.75	93	7
Cat-1	97	3

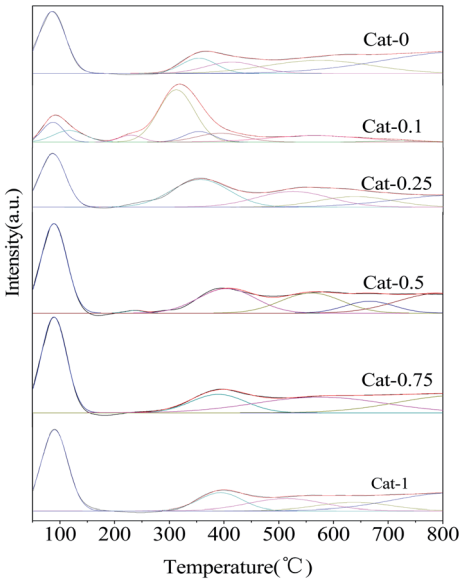

Fig. 4 Profiles of CO_2-TPD for catalysts Cat-0, Cat-0.1, Cat-0.25, Cat-0.5, Cat-0.75 and Cat-1.

Table 2 Distribution of different types of base sites on the catalyst

Catalyst	Weak/all	Middle/all (%)	Strong/all (%)
Cat-0	21	15	64
Cat-0.1	22	62	16
Cat-0.25	21	25	54
Cat-0.5	33	19	48
Cat-0.75	32	13	55
Cat-1	32	12	56

Table 3 Phosphorus content in Cat-*n* catalysts

Catalyst	Cat-0.1	Cat-0.25	Cat-0.5	Cat-0.75	Cat-1
C_P (mg L^{-1})	14.82	10.87	10.26	10.30	10.22

and the last one located around 500–700 °C can be attributed to strong base sites. With the increase of the concentration of K_3PO_4 solution, the middle base sites shift toward higher temperature, which indicates that the middle base strength of the catalyst is enhanced by increasing the concentration of K_3PO_4 solution. The peak area of TPD curve is a function of the amount of acid/base sites.[31] By integrating the peak areas of different types of base sites distributed in the three regions (weak base, middle base and strong base) in each catalyst respectively, and calculating the percentage of the amount of weak, middle or strong base sites in total base sites, the final results are summarized in Table 2. It is found that when the concentration of the K_3PO_4 solution were 0.1 mol L^{-1} and 0.25 mol L^{-1}, the middle base sites and strong base sites account for the largest proportion in total base sites respectively. With the concentration of K_3PO_4 solution increasing, the percentage of the amount of the middle base sites decreased. That might because the lower concentration of K_3PO_4 solution could combine better with NaX to improve alkalinity and alkali content of the catalyst significantly, which is consistent with the XRD analysis.

3.1.4 Determination of phosphorus content. The content of phosphorus in all the catalysts was determined by Water Quality – Determination of Phosphorus – Ammonium Molybdate Spectrometric Method (ISO 6878-2004) as shown in Table 3. By comparing all the catalysts, it is found that when the concentration of K_3PO_4 solution was 0.1 mol L^{-1}, the phosphorus content of in the catalyst was significantly higher than the others, which suggests that the lower K_3PO_4 concentration environment is beneficial to the diffusion of PO_4^{3-} in NaX.

3.2 Catalytic reaction

A series of catalysts Cat-*n* were evaluated on fix-bed reactor for the side-chain alkylation of toluene with methanol. The catalytic reaction results were shown in Table 4, from which it could be seen that ethylbenzene and styrene are the main products, and formaldehyde is an intermediate product, accompanied by some by-products such as xylene and methane. The selectivities and yields of the main products are significantly improved over the catalysts loaded with K_3PO_4 *via* ion-exchange method. When the concentration of K_3PO_4 solution is 0.1 mol L^{-1}, the selectivity of ethylbenzene reaches the highest value (82.9%); in addition, when the K_3PO_4 solution concentration is 0.25 mol L^{-1}, the selectivity of styrene is the highest (18.1%). But when the K_3PO_4 solution concentration is more than 0.5 mol L^{-1}, the selectivity and yield of the main products (ethylbenzene and styrene) begin to decrease, the selectivity of xylene and methane start to increase at the same time.

Table 4 Catalytic performance for the side-chain alkylation of toluene with methanol over Cat-*n* series of catalysts

		Selectivity of products (%)					Yield of products (%)		
Catalyst	MET conv%	S_{EB}	S_{STY}	S_{CH_4}	S_{XY}	S_{HCHO}	Y_{EB}	Y_{STY}	$Y_{(EB+STY)}$
Cat-0	99.9	0.0	0.0	16.9	83.1	0.0	0.0	0.0	0.0
Cat-0.1	99.9	82.9	8.0	5.4	3.7	0.0	82.8	8.0	90.8
Cat-0.25	99.9	70.4	18.1	8.2	3.2	0.0	70.4	18.1	88.5
Cat-0.5	99.8	53.4	6.3	25.2	9.3	5.9	53.3	6.3	59.6
Cat-0.75	99.7	57.1	5.7	20.3	11.9	5.0	56.9	5.7	62.6
Cat-1	99.8	41.4	10.4	19.2	19.4	9.5	41.4	10.4	51.8

In order to figure out why the selectivities of ethylbenzene and styrene were much different for the same series of catalysts, the correlation analysis between the distribution of the acid and base sites and the catalytic performance was carried out as shown in Fig. 5. Herein three relative percentages of acid and base sites are introduced to depict the formation probability of phenyl cation, benzyl anion and formaldehyde. From Fig. 5a and b, the selectivity of (ethylbenzene + styrene) shows the same tendency with relative percentage of (middle base–middle acid). In contrast, the relative percentage of (middle acid–middle base) exhibits the same tendency with the selectivity of (methane + xylene). Furthermore, the percentage of [(middle base–middle acid) × strong base] has the same tendency with the selectivity of styrene as shown in Fig. 5c.

According to the above results, the mechanism for SCAT reaction was proposed as shown in Fig. 6. Toluene and methanol are sensitive to the base and acid property of catalyst. A pair of competitive activations of toluene take place on middle acid and middle base sites respectively, that is, toluene converts to phenyl cation (activation of the benzene ring of toluene) over middle acid sites while it tends to become benzyl anion (activation of the side chain of toluene) over middle base sites. The more middle base sites and the less middle acid sites present on the surface of the catalyst, the more benzyl anion will be formed. Thus the relative percentage of (middle base–middle acid) can be used to depict the formation probability of benzyl anion. Therefore it indicates that the middle base is a key requirement for the SCAT reaction. Benzyl anion will be consumed along two pathways. Part of benzyl anions will combine with methanol (raw material) to form ethylbenzene, the other part of benzyl anions will bond with formaldehyde (derived from methanol on strong base sites) to form styrene. The more strong base sites appear on the surface of catalyst, the more formaldehyde will be produced, the relative percentage of the strong base can be used to describe the formation probability of formaldehyde. In brief, the distribution of [(middle base–middle acid) × strong base] shows the same tendency

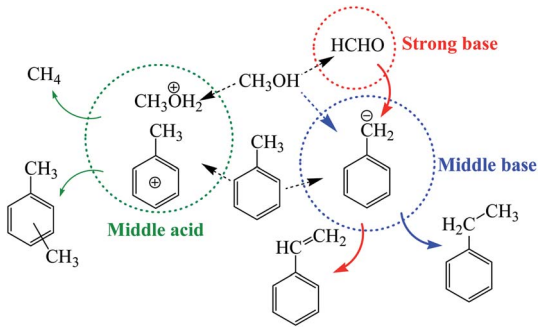

Fig. 6 The proposed reaction mechanism for SCAT reaction on the acid and base sites.

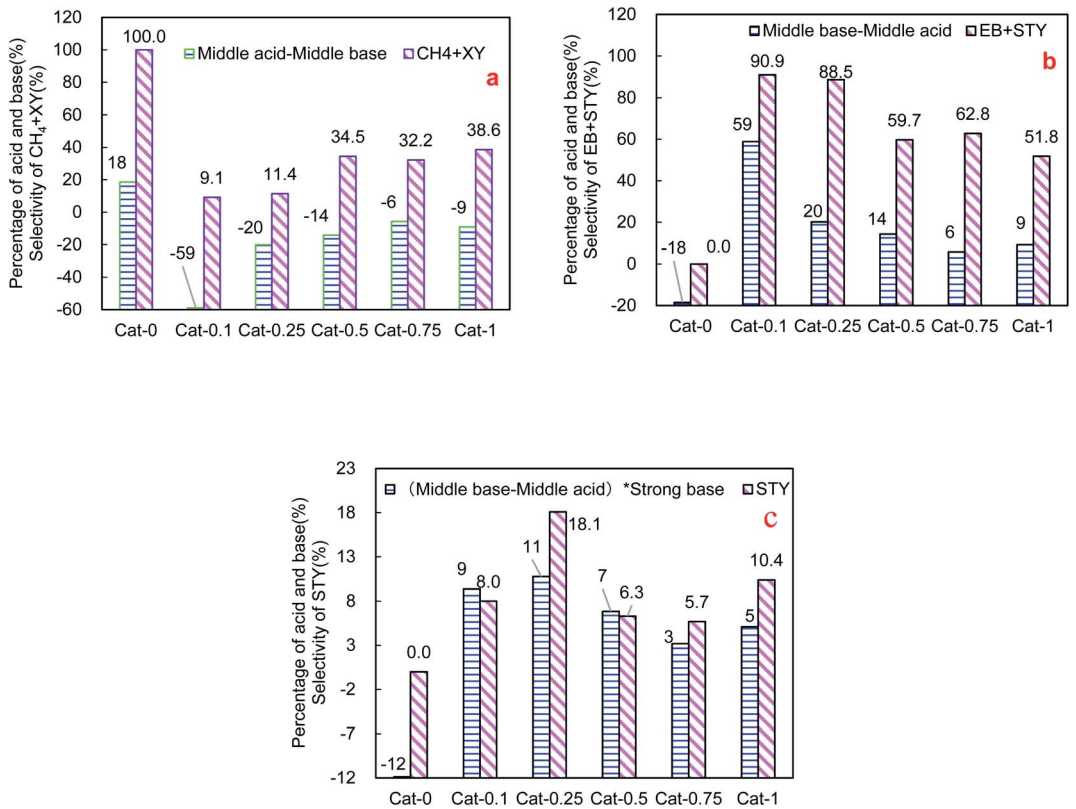

Fig. 5 Correlation analysis between relative percentages of acid and base sites and catalytic activities for Cat-*n* series of catalysts. (a) (middle acid–middle base)% *vs*. selectivity of (CH_4+XY); (b) (middle base–middle acid)% *vs*. selectivity of (EB+STY); (c) (middle acid– middle base)* strong base %) *vs*. selectivity of STY).

Table 5 Catalytic performances of Cat-0.1 and two-stage catalysts for the SCAT reaction

		Selectivity of products (%)					Yield of products (%)		
Catalyst	MET conv%	S_{EB}	S_{STY}	S_{CH_4}	S_{XY}	S_{HCHO}	Y_{EB}	Y_{STY}	$Y_{(EB+STY)}$
Cat-0.1	99.9	82.9	8.0	5.4	3.7	0.0	82.8	8.0	90.8
3%KOH/Cat-0.1	99.7	60.0	17.8	3.1	19.0	0.0	59.9	17.8	77.6
5%KOH/Cat-0.1	99.9	45.3	42.4	0.9	11.5	0.0	45.2	42.4	87.6

with the styrene selectivity changing for the Cat-*n* series of catalysts as shown in Fig. 5c.

In order to verify the strong base sites that could promote the side-chain alkylation of toluene with methanol to form styrene, a series of co-catalysts *m*%KOH/NaX were prepared and placed in front of Cat-0.1, where there are abundant middle base sites, and separated by quartz wool. Under the same catalytic reaction condition the catalytic performance for the SCAT reaction are showed in Table 5. Compared to Cat-0.1, the selectivity of styrene is enhanced significantly after introducing co-catalysts in. When the co-catalyst is replaced by 5 wt% KOH/Cat-0.1, the selectivity of styrene reaches 42.4%, which suggests that the sufficient middle and strong base sites are the key factors for the SCAT reaction to styrene.

4 Conclusions

From the characterization of the catalysts, NaX exchanged with potassium phosphate solution can obviously improve the catalytic activity and the selectivity of ethylbenzene and styrene for the SCAT reaction. Toluene and methanol are very sensitive to the base and acid property of the catalysts, that is different and competitive activations will take place for toluene and methanol over middle acid and middle base sites respectively. More middle base sites and less middle acid sites on the surface of the catalyst are beneficial to forming ethylbenzene and styrene. Furthermore, more strong base sites are in the favor of producing formaldehyde; if the middle base sites are enough exactly at the right moment, the selectivity of styrene will be greatly enhanced. That is, the enough middle and strong base sites are both necessary for the SCAT reaction to prepare styrene.

Conflicts of interest

There are no conflicts to declare.

Acknowledgements

The authors are grateful to the financial support from the National Key Technology Research & Development Program (Grant No. 2013BAC14B04), the National Natural Science Foundation of China (Grant No. 21336006), the Shanxi Province Key Research & Development Program (International Cooperation, Grant No. 201803D421099), Research Project supported by Shanxi Scholarship Council of China (Grant No. 2017-035).

References

1 Y. N. Sidorenko, P. N. Galich, V. S. Gutyrya, V. G. Ilin and I. E. Neimark, *Dokl. Akad. Nauk SSSR*, 1967, **173**, 132–134.
2 J. Jiang, G. Lu, C. Miao, X. Wu, W. Wu and Q. Sun, *Microporous Mesoporous Mater.*, 2013, **167**, 213–220.
3 A. E. Palomares, G. Eder-Mirth and J. A. Lercher, *J. Catal.*, 1997, **168**, 442–449.
4 H. Itoh, A. Miyamoto and Y. Murakami, *J. Catal.*, 1980, **64**, 284–294.
5 A. Philippou and M. W. Anderson, *J. Am. Chem. Soc.*, 1994, **116**, 5114–5183.
6 H. Hattori, *Appl. Catal., A*, 2015, **504**, 103–109.
7 J. M. Serra, A. Corma, D. Farrusseng, L. Baumes, C. Mirodatos, C. Flego and C. Perego, *Catal. Today*, 2003, **81**, 425–436.
8 H. Han, M. Liu, X. W. Nie, F. S. Ding, Y. R. Wang, J. J. Li, X. W. Guo and C. S. Song, *Microporous Mesoporous Mater.*, 2016, **234**, 61–72.
9 P. Kovacheva, A. Predoeva, K. Arishtirova and S. Vassilev, *Appl. Catal., A*, 2002, **223**, 121–128.
10 T. Zhang, J. Hu and S. W. Tang, *Chin. J. Chem. Eng.*, 2018, **26**, 1513–1521.
11 M. L. Unland and G. E. Baker, *US Pat.*, 4115424, Sep 19, 1978.
12 C. Lacroix, A. Deluzarche, A. Kiennemann and A. Boyer, *Zeolites*, 1984, **4**, 109–111.
13 L. L. Song, Y. Yu, Z. R. Li, S. Q. Guo, L. F. Zhao and W. Li, *J. Braz. Chem. Soc.*, 2014, **25**, 1346–1354.
14 N. K. Das and K. Pramanik, *J. Indian Chem. Soc.*, 1997, **74**, 701–704.
15 H. Hattori, A. A. Amusa, R. B. Jermy, A. M. Aitani and S. S. Al-Khattaf, *J. Mol. Catal. A: Chem.*, 2016, **424**, 98–105.
16 B. B. Tope, W. O. Alabi, A. M. Aitani, H. Hattori and S. S. Al-Khattaf, *Appl. Catal., A*, 2012, **443**, 214–220.
17 W. O. Alabi, B. B. Tope, R. B. Jermy, A. M. Aitani, H. Hattori and S. S. Al-Khattaf, *Catal. Today*, 2014, **226**, 117–123.
18 J. Z. Yin, Z. Ma, Z. Y. Shang, D. P. Hu and Z. L. Xiu, *Fuel*, 2012, **93**, 284–287.
19 Y. S. Choi, H. Kim, S. H. Shin, M. Cheong, Y. J. Kim, H. G. Jang, H. S. Kim and J. S. Lee, *Appl. Catal., A*, 2014, **144**, 317–324.
20 H. H. Wang, B. Wang, Y. L. Wen and W. Huang, *Catal. Lett.*, 2017, **147**, 161–166.
21 N. Jiang, H. Jin, E. Y. Jeong and S. E. Park, *J. Nanosci. Nanotechnol.*, 2010, **10**, 227–232.

22 H. L. Chen, J. Ding and Y. M. Wang, *Acta Phys.-Chim. Sin.*, 2013, **29**, 1035–1040.
23 J. M. Lee, Y. J. Min, K. B. Lee, S. G. Jeon, J. G. Na and H. J. Ryu, *Langmuir*, 2010, **26**, 18788–18797.
24 R. Manivannan and A. Panduranggan, *Catal. Lett.*, 2002, **81**, 119–124.
25 B. Wang, W. Huang, Y. L. Wen, Z. J. Zuo, Z. H. Gao and L. H. Yin, *Catal. Today*, 2011, **173**, 38–43.
26 B. Wang, W. Huang and Y. Wen, *Energy Sources, Part A*, 2011, **33**, 1933–1939.
27 H. H. Chen, X. C. Li, G. Q. Zhao, H. B. Gu and Z. R. Zhu, *Chin. J. Catal.*, 2015, **36**, 1726–1732.
28 M. D. Sefcik, *J. Am. Chem. Soc.*, 1979, **101**, 2164–2170.
29 C. Flego, G. Cosentino and M. Tagliabue, *Appl. Catal., A*, 2004, **270**, 113–120.
30 M. Yuan, M. Tan, G. Yan and J. Tao, *Chin. J. Process Eng.*, 2009, **9**, 1210–1215.
31 E. Diaz, E. Munoz, A. Vega and S. Ordonez, *Chemosphere*, 2008, **70**, 1375–1382.